Instability of Square Planar N_3-Ligand Iridium(I) Ethene Complexes

Simone Thewissen, Maike D. M. Reijnders, Jan M. M. Smits, and Bas de Bruin*

Department of Molecular Materials, Institute for Molecules and Materials, University of Nijmegen, Toernooiveld 1, NL-6525 ED Nijmegen, The Netherlands

Received July 14, 2005

New, five-coordinate, iridium(I) bis-ethene complexes [*fac*-(bpa-R)Ir^I(ethene)$_2$]$^+$ (**1**$^+$: R = H, **2**$^+$: R = Me, **3**$^+$: R = Bz; bpa-H = *N*,*N*-di(2-pyridylmethyl)amine, bpa-Me = *N*-methyl-*N*,*N*-di(2-pyridylmethyl)amine, bpa-Bz = *N*-benzyl-*N*,*N*-di(2-pyridylmethyl)amine) were prepared. In contrast to their previously reported rhodium analogues, these iridium species do not readily lose one of their two ethene fragments to form square planar mono-ethene complexes [*mer*-(bpa-R)Ir^I(ethene)]$^+$. Heating complex **1**$^+$ results in N−H activation at the bpa-H ligand and formation of the dinuclear iridium(III) species [{(*mer*-μ_2-bpa$^\#$)Ir^{III}(ethyl)-(MeCN)}$_2$]$^{2+}$ (**4**$^{2+}$) with bridging amides (bpa$^\#$ = bpa-H deprotonated at NH_{amine}). Heating bpa-Bz complex **3**$^+$ results in aromatic C−H activation of the ligand benzyl group to form dinuclear iridium(III) species [{(bpa-Bz$^\#$)Ir^{III}(μ_2-H)}$_2$]$^{2+}$ (**5**$^{2+}$) with unsupported hydride bridges (bpa-Bz$^\#$ = bpa-Bz cyclometalated at the benzylic C2-position). The dimeric structure of **5**$^{2+}$ easily breaks up in MeCN, giving the mononuclear species [(bpa-Bz$^\#$)Ir^{III}(H)(MeCN)]$^+$ (**6**$^+$). Complex **5**$^{2+}$ is also light-sensitive: glass-filtered daylight converts it to a geometrical isomer, **7**$^{2+}$, in which the cyclometalated benzyl functionality of one of the two ligands has switched its position with a pyridyl donor.

Introduction

Rh^I and Ir^I d^8 transition metals commonly adopt a 16 VE (valence electron) four-coordinate square planar coordination geometry.[1] However, 18 VE five-coordinate square pyramidal or trigonal bipyramidal geometries are also relatively abundant. Observation of five-coordinate species in solution is usually associated with chelating olefins, chelating donor ligands, and/or donor ligands that do not allow formation of a square planar geometry because of geometrical constraints. The strictly facially coordinating tri-aza-cyclononanes,[2−7] tri-thia-cyclononanes,[8−10] and tris-pyrazolylmethanes and tris-pyrazolylborates[11−18] are examples of such ligands

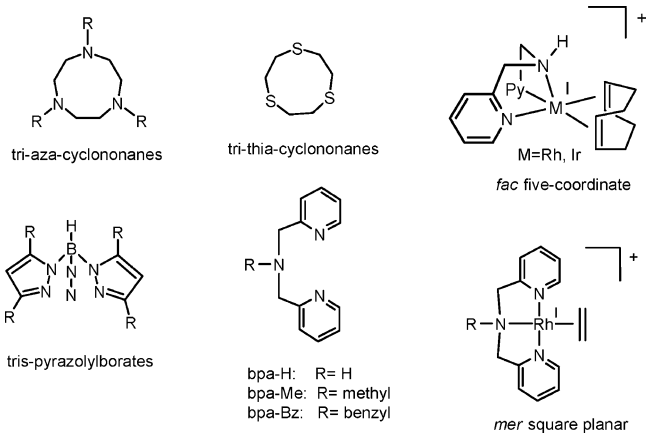

Figure 1. Rigid podal ligands and the flexible coordination modes of bpa-R ligands.

"forcing" five-coordinate geometries. The bpa-R ligands used in this paper (R = H, Me, Bz; see Figure 1) are more flexible. Like tris-pyrazolylborates, they can adopt both κ^2 and κ^3 coordination modes, but unlike trispyrazolylborates they can coordinate in both facial and meridional κ^3 modes.

* To whom correspondence should be addressed. Fax: +31 24 355 34 50. E-mail: B.deBruin@science.ru.nl.

(1) Housecroft, C. E.; Sharpe, A. G. *Inorganic Chemistry, second edition*; Pearson Education Limited: Edinburgh, 2005.
(2) de Bruin, B.; Brands, J. A.; Donners, J. J. J. M.; Donners, M. P. J.; de Gelder, R.; Smits, J. M. M.; Gal, A. W.; Spek, A. L. *Chem.−Eur. J.* **1999**, *5* (10), 2921−2936.
(3) Baker, M. V.; Brown, D. H.; Skelton, B. W.; White, A. H. *J. Chem. Soc., Dalton Trans.* **2002**, 2595.
(4) Baker, M. V.; Brown, D. H.; Skelton, B. W.; White, A. H. *J. Chem. Soc., Dalton Trans.* **2000**, 4607.
(5) Flood, T. C.; Iimura, M.; Perotti, J. M.; Rheingold, A. L.; Concolino, T. E. *Chem. Commun.* **2000**, 1681.
(6) de Bruin, B.; Donners, J. J. J. M.; de Gelder, R.; Smits, J. M. M.; Gal, A. W. *Eur. J. Inorg. Chem.* **1998**, 401.
(7) Gott, A. L.; McGowan, P. C.; Temple, C. N. *Dalton Trans.* **2004**, 1841, and references therein.
(8) Blake, A. J.; Halcrow, M. A.; Schroder, M. *Chem. Commun.* **1991**, 253.
(9) Blake, A. J.; Gould, R. O.; Halcrow, M. A.; Schroder, M. *J. Chem. Soc., Dalton Trans.* **1994**, 2197.
(10) Blake, A. J.; Halcrow, M. A.; Schroder, M. *J. Chem. Soc., Dalton Trans.* **1994**, 1631, and references therein.
(11) Trofimenko, S. *Chem. Rev.* **1993**, *93*, 943−980.
(12) Kitajima, N.; Tolman, W. B. *Prog. Inorg. Chem.* **1995**, *43*, 419.
(13) Albinati, A.; Bovens, M.; Rüegger, H.; Venanzi, L. M. *Inorg. Chem.* **1997**, *36*, 5991.
(14) Oldham, W. J., Jr.; Heinekey, D. M. *Organometallics* **1997**, *16*, 467.
(15) Esteruelas, M. A.; Oro, L. A.; Apreda, M. C.; Foces-Foces, C.; Cano, F. H.; Claramunt, R. M.; Lopez, C.; Elguero, J.; Begtrup, M. *J. Organomet. Chem.* **1988**, *344*, 93.
(16) Boutry, O.; Gutiérrez, E.; Monge, A.; Nicaso, M. C.; Pérez, P. J.; Carmona, E. *J. Am. Chem. Soc.* **1992**, *114*, 7288.
(17) Ciriano, M. A.; Fernández, M. J.; Modegro, J.; Rodríguez, M. J.; Oro, L. A. *J. Organomet. Chem.* **1993**, *443*, 249.
(18) Nicasio, M. C.; Paneque, M.; Pérez, P. J.; Pizzano, A.; Poveda, M. L.; Rey, L.; Sirol, S.; Taboada, S.; Trujillo, M.; Monge, A.; Ruiz, C.; Carmona, E. *Inorg. Chem.* **2000**, *39*, 180, and references therein.

10.1021/om050594k CCC: $30.25
Publication on Web 10/25/2005

Scheme 1. Radical Type Behavior of Ir^{II}(olefin) Species

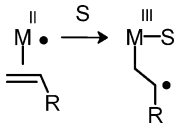

We previously described the coordination modes of bpa-R ligands to $[Rh^I(cod)]^+$, $[Ir^I(cod)]^+$ (cod = *Z*,*Z*-1,5-cyclooctadiene), and $[Rh^I(ethene)]^+$ fragments. Reaction of bpa-R ligands with $[\{(\mu_2\text{-Cl})M^I(cod)\}_2]$ resulted in formation of five-coordinate species $[(bpa\text{-}R)M^I(cod)]^+$, in which the bpa-R ligand adopts a κ^3-*fac* bpa-R coordination mode.[2,19,20] Reaction of bpa-R ligands with $[\{(\mu_2\text{-Cl})Rh^I(ethene)_2\}_2]^+$ however resulted in loss of ethene and formation of square planar $[(bpa\text{-}R)Rh^I(ethene)]^+$ complexes in which the bpa-R ligand coordinates in a κ^3-*mer* mode (see Figure 1).[21] Such $[(bpa\text{-}R)M^I(ethene)]^+$ species are potential catalysts for olefin oxygenation,[21] which explains our interest in the iridium analogues.

We were further inspired to prepare these species by our recent investigations concerning the unusual radical type behavior of organometallic iridium(II)-olefin species.[22] An intriguing aspect of this chemistry concerns our recent discovery that the unpaired spin-density is not located solely on the metal. Upon solvent coordination, a large amount of the spin-density is transferred from the metal to the "redox noninnocent" olefinic substrate (Scheme 1).[22c,d] This allows direct radical reactions at the olefin.

The significance of these new insights needs to be further established, and therefore we took an interest in square planar $[(bpa\text{-}R)Ir^I(ethene)]^+$ precursors to prepare unsaturated analogues. In attempts to prepare these species, we discovered that the square planar $[(bpa\text{-}R)M^I(ethene)]^+$ coordination geometry is not stable for iridium. Access to these species is prevented by the reactions described in this paper.

Results and Discussion

Reaction of the bpa-R ligands (R = H, Me, Bz) with in situ-generated $[(C_2H_4)_4Ir^I(Cl)]$[23] in MeOH results in formation of the cationic bis-ethene complexes $[(bpa\text{-}H)Ir^I(C_2H_4)_2]^+$ (**1**$^+$), $[(bpa\text{-}Me)Ir^I(C_2H_4)_2]^+$ (**2**$^+$), and $[(bpa\text{-}Bz)Ir^I(C_2H_4)_2]^+$ (**3**$^+$). See Figure 2.

^{1}H NMR data of **1**$^+$, **2**$^+$, and **3**$^+$ reveal two equivalent N-C*H*$_2$-Py groups. As expected, the diastereotopic N-C*H*$_2$-Py methylene protons (H_{ax}, H_{eq}, see Figure 2) give rise to an AB pattern. The two ethene molecules are inequivalent, and each reveals two triplet-like signals in ^{1}H NMR, indicating that the ethene fragments do not rotate rapidly on the NMR time-scale. For each complex, one of these ethene fragments reveals intense NOE contacts with the amine-R group in the ^{1}H-NOESY spectra. This ethene fragment gives rise to broader ^{1}H NMR signals, which indicates that this fragment is somewhat more fluxional and perhaps less strongly coordinated to the iridium center than the other ethene fragment.

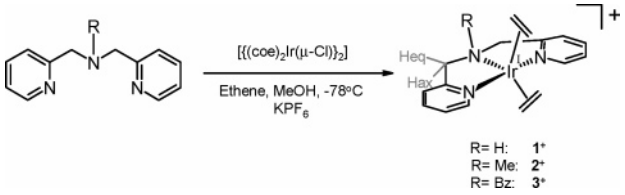

Figure 2. Synthesis of $[(\kappa^3\text{-}bpa\text{-}R)Ir^I(C_2H_4)_2]^+$ (R = H, Me, Bz).

The other NOE contacts in the ^{1}H-NOESY spectrum are indicative of a *mer* coordination mode of the bpa-R ligands. The methylene H_{eq} signal reveals NOE contacts with both Py-*H3* and the broadened signal of the ethene fragment close to the R group of the bpa-R ligand. The methylene H_{ax} signal reveals NOE contacts with another ethene fragment (the one revealing sharp ^{1}H NMR signals). The Py-*H6* signal reveals NOE contacts with both ethene fragments. From these observations we propose the trigonal-bipyramidal coordination geometries shown in Figure 2. The trigonal plane is formed by the two ethene molecules and the amine-N donor. The axial positions are taken by the pyridyl donors. This structure is similar to that observed for the analogous complexes $[(\kappa^3\text{-}mer\text{-}tpa)Ir^I(ethene)_2]^+$ and $[(i\text{Pr-pybox})Ir^I(ethene)_2]^+$,[24,25] but differs from the sterically more hindered Me_2-bpa-Me and Me_3-tpa complexes $[(\kappa^3\text{-}fac\text{-}Me_2\text{-}bpa\text{-}Me)Ir(ethene)_2]^+$ and $[(\kappa^3\text{-}fac\text{-}Me_3\text{-}tpa)Ir(ethene)_2]^+$, in which the ligands adopt a facial coordination mode.[26]

All three iridium(I) bis-ethene complexes are quite stable in solution at rt under an inert atmosphere. Bubbling nitrogen through a solution for about 30 min does not result in ethene dissociation. Upon heating a solution of the bpa-Me complex **2**$^+$, no reaction was observed at all. This bis-ethene complex is apparently very stable. Heating the bpa-H and bpa-Bz complexes **1**$^+$ and **3**$^+$ also does not result in formation of the expected square planar $[(bpa\text{-}R)Ir^I(C_2H_4)]^+$ (R = H, Bz) complexes. Instead these species escape via the follow-up reactions described below.

Reactivity of bpa-H Iridium(I) Bis-ethene upon Heating: N−H Activation. Heating a solution of bpa-H iridium(I) bis-ethene complex **1**$^+$ in CD_3CN to about 70 °C for 2 h results in formation of the dinuclear iridium(III) ethyl complex **4**$^{2+}$ (see Figure 3). The same reaction at room temperature requires about 20 days. According to ^{1}H NMR, no byproducts are formed.

(19) de Bruin, B.; Budzelaar, P. H. M.; Gal, A. W. *Angew. Chem., Int. Ed.* **2004**, *43* (32), 4142−4157.

(20) de Bruin, B.; Boerakker, M. J.; Donners, J. J. J. M.; Christiaans, B. E. C.; Schlebos, P. P. J.; de Gelder, R.; Smits, J. M. M.; Spek, A. L.; Gal, A. W. *Angew. Chem., Int. Ed.* **1997**, *36* (19), 2064−2067.

(21) de Bruin, B.; Verhagen, J. A. W.; Schouten, C. H. J.; Gal, A. W.; Feichtinger, D.; Plattner, D. A. *Chem.−Eur. J.* **2001**, *7* (2), 416−422.

(22) (a) de Bruin, B.; Peters, T. P. J.; Thewissen, S.; Blok, A. N. J.; Wilting, J. B. M.; de Gelder, R.; Smits, J. M. M.; Gal, A. W. *Angew. Chem., Int. Ed.* **2002**, *41* (12), 2135−2138. (b) de Bruin, B.; Thewissen, S.; Yuen, T.-W.; Peters, T. P. J.; Smits, J. M. M.; Gal, A. W. *Organometallics* **2002**, *21*, 4312−4314. (c) Hetterscheid, D. G. H.; Kaiser, J.; Reijerse, E.; Peters, T. P. J.; Thewissen, S.; Blok, A. N. J.; Smits, J. M. M.; de Gelder, R.; de Bruin, B. *J. Am. Chem. Soc.* **2005**, *127*, 1895−1905. (d) Hetterscheid, D. G. H.; Bens, M.; de Bruin, B. *Dalton Trans.* **2005**, 979−984.

(23) Onderlinden, A. L.; van der Ent, A. *Inorg. Chim. Acta* **1972**, *6*, 420−426.

(24) Krom, M.; Peters, T. P. J.; Coumans, R. G. E.; Sciarone, T. J. J.; Hoogboom, J.; ter Beek, S. I.; Schlebos, P. P. J.; Smits, J. M. M.; de Gelder, R.; Gal, A. W. *Eur. J. Inorg. Chem.* **2003**, *6*, 1072−1087.

(25) Díez, J.; Gamasa, M. P.; Gimeno, J.; Paredes, P. *Organometallics* **2005**, *24*, 1799.

(26) de Bruin, B.; Peters, T. P. J.; Wilting, J. B. M.; Thewissen, S.; Smits, J. M. M.; Gal, A. W. *Eur. J. Inorg. Chem.* **2002**, *10*, 2671−2680.

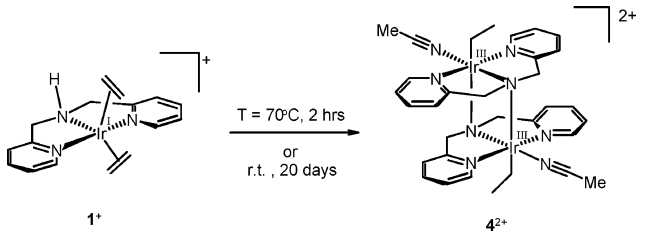

Figure 3. Formation of $\mathbf{4}^{2+}$ from $\mathbf{1}^{+}$.

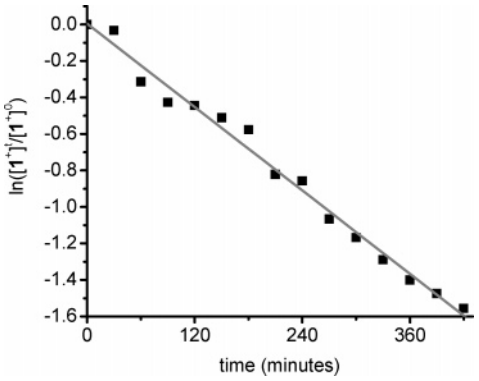

Figure 4. Plot of $\ln([\mathbf{1}^{+}]^t/[\mathbf{1}^{+}]^0)$ vs time in the conversion of $\mathbf{1}^{+}$ to $\mathbf{4}^{2+}$ showing first-order kinetics in $\mathbf{1}^{+}$.

Complex $\mathbf{4}^{2+}$ proves to be air stable in solution. This complex must have formed from $\mathbf{1}^{+}$ by deprotonation of the amine-nitrogen of the bpa-H ligand (to give bpa$^{\#}$), allowing formation of a bridging amide functionality.

When the reaction is carried out in CH_3CN, solvent coordination is clearly recognized by a ^{1}H NMR signal at 2.70 ppm. Upon dissolving the CH_3CN-coordinated complex in CD_3CN, no exchange between coordinated CH_3CN and the solvent takes place, indicating a very strong bond between the iridium(III) center and the nitrile.

^{1}H-NOE contacts are characteristic of a dinuclear complex with a *mer*-coordination mode of the deprotonated bpa-ligand with the ethyl group at a position *cis* to the two pyridyl donors and the N_{amide}. Furthermore, strong NOE contacts between one of the N-C*H*$_2$-Py methylene protons and two of the pyridine protons (Py-*H3* and -*H6*) are observed, which confirm the dinuclear nature of the complex.

When the reaction is carried out in pure CD_3CN, $\mathbf{4}^{2+}$ is obtained without incorporation of any deuterium atoms at the ethyl moiety. In contrast, H/D exchange at the N*H*$_{amine}$ position of $\mathbf{1}^{+}$ occurs almost instantaneously in a mixture of CD_3CN and CD_3OD, yielding $\mathbf{1}^{+}$-D (containing the ligand bpa-D). Heating a sample of thus obtained $\mathbf{1}^{+}$-D in CD_3CN leads to formation of $\mathbf{4}^{2+}$-D_2, containing two monodeuterated ethyl fragments $-CH_2CH_2D$, as indicated by ^{1}H NMR. Therefore, the proton used to convert the olefin into an ethyl group must stem from the N*H*$_{amine}$ fragment.

The rate of formation of complex $\mathbf{4}^{2+}$ from $\mathbf{1}^{+}$ at 40 °C was followed by ^{1}H NMR (Figure 4). Plots of $\ln([\mathbf{1}^{+}]^t/[\mathbf{1}^{+}]^0)$ vs time result in straight lines, characteristic of first-order kinetics in $\mathbf{1}^{+}$. The kinetic data are clearly inconsistent with second-order kinetics associated with rate-determining *inter*molecular N−H activation or bridge formation steps. Considering the above-described rapid H/D exchange, the NH_{amine} fragment (which strongly resembles an ammonium ion) must be rather acidic, and it thus seems also unlikely that breaking of this weak N−H bond would be rate determining. Considering the fact that we never observed a monoethene intermediate, rate-limiting ethene dissociation from $\mathbf{1}^{+}$ provides a plausible explanation for the observed first-order kinetics.

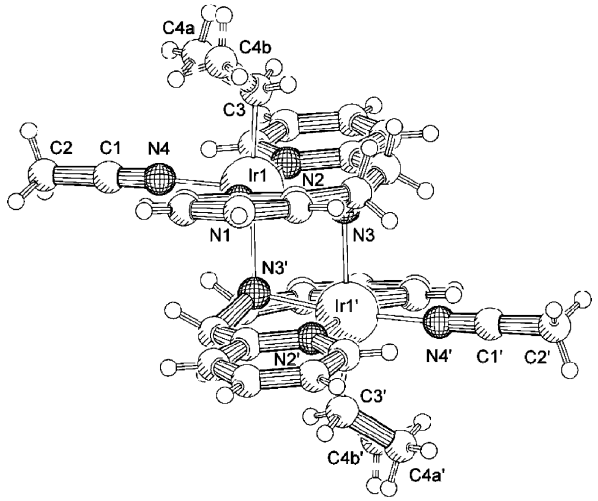

Figure 5. X-ray structure of $\mathbf{4}^{2+}$.

We thus propose that formation of $\mathbf{4}^{2+}$ involves dissociation of one of the ethene fragments to give a reactive four-coordinate iridium(I) complex. The subsequent (*inter*- or *intra*molecular) N−H activation of the bpa-H ligand seems to be relatively fast. Since the NH_{amine} fragment of $\mathbf{1}^{+}$ is rather acidic, the ethyl formation might well involve protonation of (solvated) Ir^{I}(ethene) species by N*H*$_{amine}$, either directly at ethene or via an Ir^{III}-hydride species, to form an Ir^{III}(ethyl) fragment.[27]

Crystals suitable for X-ray diffraction were obtained by vapor diffusion of diethyl ether into a solution of $\mathbf{4}(PF_6)_2$ in acetonitrile. The X-ray structure of $\mathbf{4}^{2+}$ is shown in Figure 5. Selected bond lengths and angles are given in Table 1. Unfortunately, during the X-ray measurement the crystals decomposed due to evaporating solvent molecules from the lattice, which degraded the quality of the measurements.

The dinuclear iridium complex $\mathbf{4}^{2+}$ has an inversion center and a slightly distorted octahedral geometry around each metal center with the N_3 ligand still coordinated in a meridional fashion. The MeCN ligands are coordinated in the plane of the *mer*-bpa$^{\#}$ ligand, *cis* to the pyridyl donors. The ethyl group occupies an axial position, *cis* to the pyridyl and MeCN donors. The end-of-chain carbon of the ethyl group (atom C4) is disordered. The pyridine rings are positioned in such a way that π-stacking between the two N_3 ligands is optimal, which could be one of the driving forces for the reaction.

Reactivity of bpa-Bz Iridium(I) Bis-ethene upon Heating: C−H Activation. Heating a saturated solution of $[(\text{bpa-Bz})\text{Ir}^{I}(\text{ethene})_2]^{+}$ complex $\mathbf{3}^{+}$ in acetone for 24 h at 50 °C results in precipitation of pure complex

(27) For similar protonation reactions see: (a) de Bruin, B.; Boerakker, M. J.; Verhagen, J. A. W.; de Gelder, R.; Smits, J. M. M.; Gal, A. W. *Chem. Eur. J.* **2000**, *6* (2), 298−312. (b) Brookhart, M.; Lincoln, D. M.; Bennet, M. A.; Pelling, S. *J. Am. Chem. Soc.* **1990**, *112*, 2691. (b) Öhrström, L.; Strömberg, S.; Glaser, J.; Zetterberg, K. *J. Organomet. Chem.* **1998**, *558*, 123. (c) Ciriano, M. A.; Fernández, M. J.; Modegro, J.; Rodríguez, M. J.; Oro, L. A. *J. Organomet. Chem.* **1993**, *443*, 249, and references therein.

Table 1. Selected Bond Lengths and Angles of 4^{2+}

bond length (Å)		angle (deg)			angle (deg)
Ir1−N1	2.034(8)	N1−Ir1−N2	163.7(3)	N4−Ir1−C3	90.8(4)
Ir1−N2	2.011(8)	N1−Ir1−N3	83.4(3)	N3′−Ir1−N1	94.5(3)
Ir1−N3	2.036(7)	N1−Ir1−N4	98.7(3)	N3′−Ir1−N2	93.2(3)
Ir1−N4	2.014(8)	N2−Ir1−N3	83.8(3)	N3′−Ir1−N3	79.7(3)
Ir1−C3	2.113(10)	N2−Ir1−N4	95.2(3)	N3′−Ir1−C3	175.9(3)
Ir1−N3′	2.266(8)	N1−Ir1−C3	85.8(4)	Ir1−N3−Ir1′	100.3(3)
Ir−Ir1	3.305(6)	N2−Ir1−C3	85.6(4)	torsion: N1−Ir1−Ir1′−N2′	−8.40
		N3−Ir1−C3	96.2(4)		

Table 2. Selected Bond Lengths and Angles of 5^{2+}

bond length (Å)			angle (deg)
Ir1−Ir1′	2.6877(6)	N1−Ir1−C37	87.3(2)
Ir1−N1	2.043(6)	N2−Ir1−C37	86.1(2)
Ir1−N2	2.036(6)	N4−Ir1−N1	81.1(2)
Ir1−N4	2.070(6)	N4−Ir1−N2	81.8(2)
Ir1−C37	2.005(7)	N1−Ir1−N2	162.4(2)
		torsion: N1−Ir1−Ir1′−N2′	16.23

$\mathbf{5}^{2+}$ as a yellow solid. Complex $\mathbf{5}^{2+}$ is a dinuclear iridium(III) species with a cyclometalated benzyl-amine fragment and bridging hydrides (see Figure 6).

The equivalent bridging hydrides of $\mathbf{5}^{2+}$ give rise to a sharp ^{1}H NMR signal at $\delta = -14.73$ ppm in acetone-d_6. A clear indication of the dinuclear nature of the complex is obtained from NOESY experiments. NOE contacts are observed between the Py-*H6* and both the Py-*H3* and one of the *N*-CH_2-Py methylene protons. A Py-*H6* proton

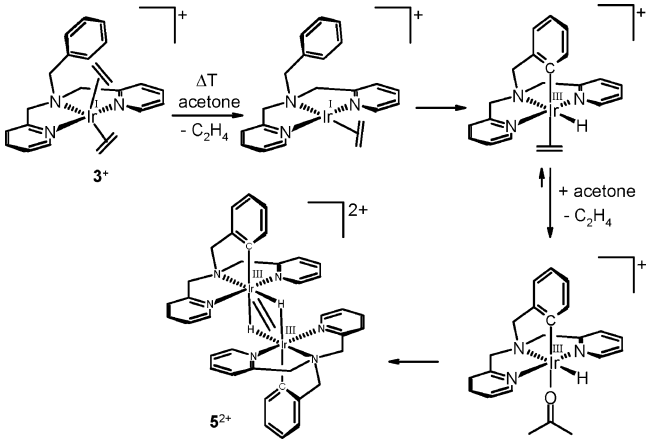

Figure 6. Proposed pathway for the formation of $\mathbf{5}^{2+}$ from $\mathbf{3}^{+}$.

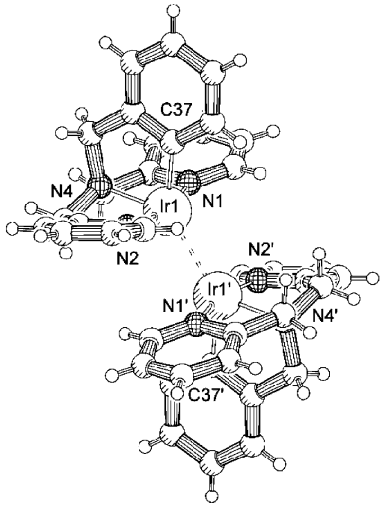

Figure 7. X-ray structure of $\mathbf{5}^{2+}$ (bridging hydrides were not located).

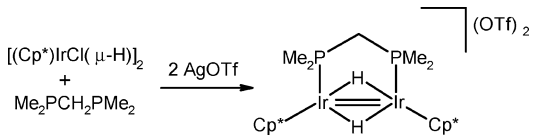

Figure 8. Dinuclear iridium complexes with bridging hydrogen atoms by Fujita et al.

can display such NOE contacts only if two N_3 ligands are in close proximity to one another (Figures 6 and 7). The cyclometalation causes an upfield shift of more than 0.7 ppm in the ^{1}H NMR for most of the aromatic benzyl signals of $\mathbf{5}^{2+}$ as compared to $\mathbf{3}^{+}$. The two pyridine rings and the N-*C*H_2-Py methylene groups show up as equivalent functionalities in the ^{1}H NMR.

Crystals of $\mathbf{5}(PF_6)_2$, suitable for X-ray diffraction, were obtained from an acetone solution of $\mathbf{3}(PF_6)$, from which $\mathbf{5}(PF_6)_2$ slowly precipitated as a crystalline material over the course of three weeks at room temperature. The X-ray structure of $\mathbf{5}^{2+}$ is shown in Figure 7. Selected bond lengths and angles are given in Table 2.

In the crystal structure, dinuclear Ir complex $\mathbf{5}^{2+}$ is located at an inversion center, with an Ir−Ir distance of 2.6877(6) Å. We were not able to locate the bridging hydrogen atoms in $\mathbf{5}^{2+}$ with X-ray diffraction.

Short Ir−Ir contacts bridged solely by hydrides are uncommon, but some examples of (poly)hydride-bridged iridium complexes are known.[28−32] Hydrogen-bridged dinuclear iridium(III) complexes containing additional diphosphine bridges were reported by Fujita et al.[33−35] For these complexes (Figure 8) the bridging hydrogen atoms are observed at $\delta = -17.82$ ppm in acetone-d_6.

Addition of acetylene to this dinuclear iridium hydride complex gives a μ-vinyl complex, $[(Cp^*Ir)_2(\mu\text{-dmpm})(\mu^2,\eta^1,\eta^2\text{-CH=CH}_2)(\mu\text{-H})]^{2+}$, via addition of one of the iridium hydrides to the carbon−carbon triple bond. In this complex the bridging hydride is found at $\delta = -20.36$ ppm (in acetone-d_6). When *tert*-butylisocyanide is added, one of the iridium−hydride bonds is broken and the isocyanide coordinates to one of the iridium centers. The chemical shift of the bridging hydride in this case is

(28) Taw, F. L.; Mellows, H.; White, P. S.; Hollander, F. J.; Bergman, R. G.; Brookhart, M.; Heinekey, D. M. *J. Am. Chem. Soc.* **2002**, *124* (18), 5100−5108.
(29) Chen, M. J.; Nunez, L.; Rathke, J. W.; Rogers, R. D. *Organometallics* **1996**, *15* (9), 2338−2344.
(30) Schnabel, R. C.; Carroll, P. S.; Roddick, D. M. *Organometallics* **1996**, *15* (2), 655−662.
(31) Heinekey, D. M.; Fine, D. A.; Harper, T. G. P.; Michel, S. T. *Can. J. Chem.−Rev. Can. Chim.* **1995**, *73* (7), 1116−1125.
(32) Robertson, G. B.; Tucker, P. A. *Austr. J. Chem.* **1984**, *37* (2), 257−263.
(33) Fujita, K.; Hamada, T.; Yamaguchi, R. *J. Chem. Soc., Dalton Trans.* **2000**, *12*, 1931−1936.
(34) Fujita, K.; Nakaguma, H.; Hamada, T.; Yamaguchi, R. *J. Am. Chem. Soc.* **2003**, *125* (41), 12368−12369.
(35) Fujita, K.; Nakaguma, H.; Hanasaka, F.; Yamaguchi, R. *Organometallics* **2002**, *21* (18), 3749−3757.

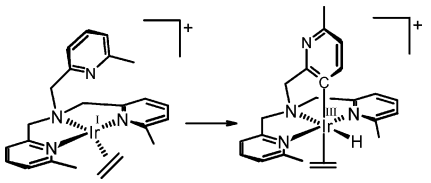

Figure 9. C−H activation of a pyridyl donor in a Me_3-tpa iridium(I) ethene complex.

−24.00 ppm and that of the terminal hydride is −15.51 ppm (in CD_2Cl_2).

From the above data it is clear that heating complex $\mathbf{3}^+$ leads to cyclometalation of the bpa-Bz benzyl functionality. The poor solubility of the product $\mathbf{5}^{2+}$, and its immediate precipitation upon formation, severely hampers any kinetic measurements for this reaction. Therefore we can only speculate about the mechanism of this reaction. As in the formation of $\mathbf{4}^{2+}$, we propose that, prior to cyclometalation, dissociation of one of the ethene fragments occurs to give a reactive four-coordinate iridium(I) complex. Apparently iridium activates the aromatic C−H bond at the 2-position of the phenyl ring to yield a hydride species. Two of such resulting iridium(III) hydride species apparently dimerize to form the observed hydride-bridged species $\mathbf{5}^{2+}$. The ethene fragments as present in $\mathbf{3}^+$ have dissociated from the metal along this process (Figure 6).

We previously reported a similar aromatic C−H activation of a pyridyl donor for the Me_3-tpa iridium(I) ethene complex.[26] But in this case the ethene fragment remains coordinated to the metal center in acetone and no bridging hydride species are formed (Figure 9).

For $[(Me_3\text{-tpa})Ir^{I}(\text{ethene})]^+$ we proposed that pyridyl dissociation generates a monovacant trigonal-bipyramidal ethene complex.[26] The distortion from the ideal square planar geometry was thought to be the reason for the observed oxidative addition of the C−H bond at the 3-position of the pyridine ring. However, for bpa-R iridium(I) mono-ethene complexes square planar geometries would be expected on the basis of analogy with the corresponding rhodium complexes.[22] Also work by Goldberg[36−38] shows that for platinum systems a three-coordinate 14 VE metal complex is needed for oxidative addition. To what extent this is applicable to our iridium species is not clear, but at least it shows that the mechanism of aromatic C−H activation in $\mathbf{3}^+$ can be quite complicated.

Irrespective of the exact mechanism, these square planar iridium(I) mono-ethene complexes appear to be more reactive than their rhodium analogues, so that they tend to "escape" via oxidative reactions. With ^{1}H NMR, we never observed these four-coordinate N_3-ligand iridium(I) ethene species (not from $\mathbf{3}^+$, nor from $\mathbf{1}^+$ or $\mathbf{2}^+$).

To obtain a formal saturated 18 VE counting, complex $\mathbf{5}^{2+}$ should be drawn with two metal−metal bonds (see Figure 6). However, these "bonds" are not likely to have any physical or chemical meaning, and the bridge

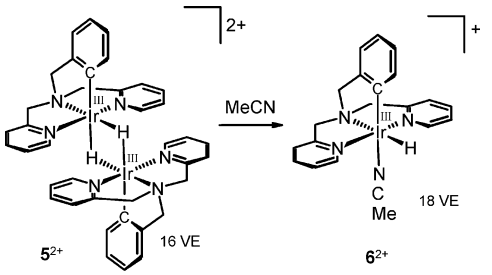

$\mathbf{5}^{2+}$ $\mathbf{6}^{2+}$

Figure 10. Reaction of $\mathbf{5}^{2+}$ in acetonitrile.

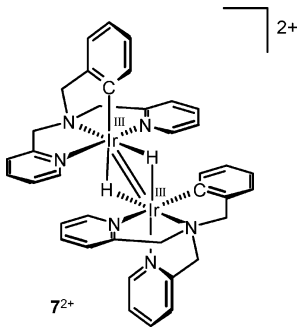

$\mathbf{7}^{2+}$

Figure 11. Proposed structure of $\mathbf{7}^{2+}$.

formation is perhaps most adequately described to be solely the result of two 3c-2e bonds, leaving each iridium center with an unsaturated formal 16 VE count (Figure 10). This is in better agreement with the observed reactivity of $\mathbf{5}^{2+}$ toward coordinating solvents.

Hydride-bridged dinuclear complex $\mathbf{5}^{2+}$ is stable in the weakly coordinating solvent acetone (in the dark), but in the coordinating solvent acetonitrile it easily converts to the acetonitrile-coordinated mononuclear iridium(III) hydride species, $[(\text{bpa-Bz}^{\#})Ir^{III}(H)(CD_3CN)]^+$ ($\mathbf{6}^+$, Figure 10). Upon dissolving $\mathbf{5}^{2+}$ in CD_3CN, the ^{1}H signal of the original dinuclear complex ($\delta = -14.73$ ppm in acetone-d_6, $\delta = -15.12$ in CD_3CN) disappears very rapidly, whereas a new hydride signal comes up at $\delta = -18.30$ ppm. Within 25 min 87% of dinuclear complex $\mathbf{5}^{2+}$ is converted to the mononuclear complex $\mathbf{6}^+$. The reaction goes to completion within an hour. On the basis of ^{1}H NMR we conclude that this yields 95% of complex $\mathbf{6}^+$ and 5% of an unknown species with a hydride signal at −18.82. This could be an isomer of $\mathbf{6}^+$, having the hydride *trans* to the metal−carbon bond. ESI$^+$-MS measurements confirm the composition of $\mathbf{6}^+$ as $[(\text{bpa-Bz}^{\#})Ir^{III}(H)(MeCN)]^+$. Complex $\mathbf{6}^+$ is stable at room temperature in CD_3CN in the presence of air.

Although $\mathbf{5}^{2+}$ is stable in acetone in the dark, it proves to be very light sensitive. As soon as an acetone solution of the complex is exposed to glass-filtered daylight, it immediately starts to convert to complex $\mathbf{7}^{2+}$. Complete conversion of symmetrical complex $\mathbf{5}^{2+}$ to asymmetrical complex $\mathbf{7}^{2+}$ requires only a few hours. On the basis of ^{1}H-COSY, ^{1}H-NOESY, and ESI$^+$-MS we propose $\mathbf{7}^{2+}$ to be the asymmetrical, dinuclear hydride-bridged species depicted in Figure 11.

Formation of $\mathbf{7}^{2+}$ stops when a solution of $\mathbf{5}^{2+}$ is no longer exposed to daylight. Upon prolonged exposure of an acetone solution of $\mathbf{7}^{2+}$ to daylight, no further rearrangements take place: the other benzyl ring remains to be coordinated in a position *trans* to one of the hydrides.

We propose that one of the Ir−H bonds breaks upon irradiation (most probably the one with the aromatic

(36) Crumpton-Bregel, D. M.; Goldberg, K. I. *J. Am. Chem. Soc.* **2003**, *125* (31), 9442−9456.

(37) Fekl, U.; Goldberg, K. I. *Homogeneous hydrocarbon C−H bond activation and functionalization with platinum*; Advances in Inorganic Chemistry: Including Bioinorganic Studies, Volume 54; Academic Press Inc.: San Diego, 2003.

(38) Jensen, M. P.; Wick, D. D.; Reinartz, S.; White, P. S.; Templeton, J. L.; Goldberg, K. I. *J. Am. Chem. Soc.* **2003**, *125* (28), 8614−8624.

Table 3. T_1 of the Hydride Signals of the bpa-Bz# Iridium(III) Hydride Complexes

compound	δ (ppm)	T_1 (ms)	δ (ppm)	T_1 (ms)
$\mathbf{5}^{2+}$ (acetone-d_6)	−14.7	650		
$\mathbf{6}^{+}$ (CD_3CN)	−18.3	2300		
$\mathbf{7}^{2+}$ (acetone-d_6)	−14.9	725	−23.89	725
$\mathbf{7}^{2+}$ (CD_3CN)	−15.0	700	−24.0	700

carbon *trans* coordinated, which is the weakest Ir−H bond due to the strong *trans*-effect of a metal−carbon fragment). Hereafter the dinuclear complex rearranges to the more stable complex $\mathbf{7}^{2+}$, in which only one of the bridging hydrides is located *trans* to a metal−carbon fragment. The ^{1}H NMR signal at $\delta = -14.90$ probably corresponds to the hydride with the carbon *trans* (only a shift of 0.2 ppm to higher field as compared to $\mathbf{5}^{2+}$). The hydride located *trans* to the N_{amine} and N_{Py} donors then appears at a chemical shift of −23.92 ppm in the ^{1}H NMR spectrum. Since the latter hydride is no longer coordinated in a position *trans* to a carbon donor, this hydride bridge will be much stronger, thus making the dinuclear complex more stable. From ESI$^+$-MS measurements it can indeed be concluded that upon spraying acetone solutions of the dicationic dinuclear complexes, fragmentation to monocationic mononuclear complexes is much easier for $\mathbf{5}^{2+}$ than for $\mathbf{7}^{2+}$.

Another indication that the bridge in $\mathbf{7}^{2+}$ is stronger compared to $\mathbf{5}^{2+}$ comes from the fact that addition of CD_3CN does not result in formation of an isomer of $\mathbf{6}^{+}$. The dinuclear complex $\mathbf{7}^{2+}$ remains intact even in pure CD_3CN solutions, as confirmed by NMR and ESI$^+$-MS measurements.

The proton spin−lattice relaxation times (T_1) were measured for $\mathbf{5}^{2+}$ (acetone-d_6), $\mathbf{6}^{+}$ (CD_3CN), and $\mathbf{7}^{2+}$ (both in acetone-d_6 and in CD_3CN). The results are shown in Table 3. From such relaxation times information about the coordination mode of the hydrides can be deduced.[39]

Since these relaxation times are mainly determined by H−H spin−spin relaxation processes, the large differences in T_1 between mononuclear complex $\mathbf{6}^{+}$ and the dinuclear complexes $\mathbf{5}^{2+}$ and $\mathbf{7}^{2+}$ are expected. For the dinuclear complexes, the H−H distance will dominate T_1. Apparently there is no large change on going from $\mathbf{5}^{2+}$ to $\mathbf{7}^{2+}$, supporting our assumption that both these complexes contain two bridging hydrides.

The hypothesis that $\mathbf{7}^{2+}$ might also be a complex with one bridging and one terminal hydride can be ruled out: in such a complex the H−H distance should have changed considerably, which should have had its impact on T_1. The fact that the T_1 values of $\mathbf{7}^{2+}$ in acetone-d_6 and in CD_3CN are similar is a further indication that the bridging structure of $\mathbf{7}^{2+}$ remains intact even in coordinating solvents such as MeCN.

Conclusions

If we compare the N_3-ligand complexes $[(\text{bpa-R})Rh^I]^+$ and $[(\text{bpa-R})Ir^I]^+$ (R = H, Me, Bz) in complexation with ethene we see some remarkable differences. Whereas the Rh complexes readily form stable four-coordinate square planar *mono*-ethene $[(\text{bpa-R})Rh^I(\text{ethene})]^+$ species,[21] the corresponding Ir complexes form stable five-coordinate *bis*-ethene species $[(\text{bpa-R})Ir^I(\text{ethene})_2]^+$. Remarkably, these do *not* easily lose one of their ethene fragments. Thermal activation leads to ethene dissociation, but this does not lead to formation of square planar $[(\text{bpa-R})Ir^I(\text{ethene})]^+$ analogues of the rhodium species. Instead, upon heating bpa-H complex $\mathbf{1}^{+}$, the presumed four-coordinate intermediate escapes via N−H activation at the NH_{amine} fragment of the bpa-H ligand, to form dinuclear species $\mathbf{4}^{2+}$ with bridging amides. Upon heating bpa-Bz complex $\mathbf{3}^{+}$, the presumed four-coordinate intermediate escapes via an aromatic C−H activation process of the aromatic benzyl fragment of the bpa-Bz ligand to form dinuclear species $\mathbf{5}^{2+}$ with bridging hydrides. Upon heating bpa-Me complex $\mathbf{2}^{+}$, no reaction was observed at all, illustrating the unusually large affinity of these complexes for both coordinated ethene fragments.

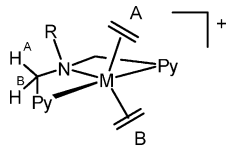

$[(\text{bpa-R})Ir(C_2H_4)_2]^+$

Figure 12. Assignment of NMR signals in $[(\text{bpa-R})Ir^I(\text{ethene})_2]^+$ complexes.

Experimental Section

General Methods. All procedures were performed under a nitrogen atmosphere using standard Schlenck techniques, unless indicated otherwise. Solvents (p.a.) were deoxygenated by bubbling through a stream of nitrogen or by the freeze−pump−thaw method. The temperature indication rt corresponds to ca. 20 °C.

NMR experiments were carried out on a Bruker DPX200 (200 and 50 MHz for ^{1}H and ^{13}C, respectively), a Bruker AC300 (300 and 75 MHz for ^{1}H and ^{13}C, respectively), and a Varian Inova 400 (400 and 100 MHz for ^{1}H and ^{13}C, respectively). Solvent shift references for ^{1}H NMR are as follows: CD_2Cl_2 δ (^{1}H) = 5.31 ppm, CD_3CN δ (^{1}H) = 1.94 ppm, methanol-d_4 δ (^{1}H) = 3.35 ppm, and acetone-d_6 δ (^{1}H) = 2.05 ppm. Solvent shift references for ^{13}C NMR are as follows: CD_3CN δ (^{13}C) = 1.24 (and 118.25), CD_2Cl_2 δ (^{13}C) = 54.20, methanol-d_4 δ (^{13}C) = 49.3 ppm, and acetone-d_6 δ (^{13}C) = 29.83 ppm (and 206.18 ppm). Abbreviations used: s = singlet, d = doublet, dd = double doublet, ddd = double doublet of doublets, t = triplet, dt = double triplet, q = quartet, qq = quartet of quartets, m = multiplet, dm = double multiplet, br = broad.

Spin−lattice relaxation times (T_1) were measured at 298 K and at 500 MHz.

Since the κ^3-bpa-R iridium(I) bis-ethene complexes have two chemically different ethene molecules (one above the trigonal plane having NOE contacts with the amine-R group (C_2H_4, A), the other below this plane (C_2H_4, B)), the NMR signals belonging to the different olefins and the diastereotopic methylene protons of the N-CH_2-Py groups are assigned as shown in Figure 12.

Elemental analyses (C, H, N) were carried out on a Carlo Erba NCSO analyzer.

Mass spectra (ESI- or FAB-MS) were recorded on a Finnigan MAT 900S (Radboud University Nijmegen) or a Finnigan TSQ 700 (ETH-Zurich). All spectra were obtained in the positive ion mode. Daughter ion spectra were measured on the TSQ 700 and TSQ 7000 using argon as a collision gas.

(39) Bakhmutov, V. I.; Vorontsov, E. V.; Nikonov, G. I.; Lemenovskii, D. A. *Inorg. Chem.* **1998**, *37* (2), 279−282.

Table 4. Crystallographic Data for $4(PF_6)_2$ and $5(PF_6)_2$

	$4(PF_6)_2$	$5(PF_6)_2 \cdot 4(CH_3)_2CO$
empirical formula	$C_{32}H_{40}F_{12}Ir_2N_8P_2$	$C_{25}H_{30}F_6Ir_1N_3O_2P_1$
cryst size [mm]	0.62 × 0.50 × 0.39	0.70 × 0.70 × 0.22
cryst color	light yellow-green	transparent brown-red
fw	1211.06	741.69
T [K]	150(2)	208(2)
cryst syst	tetragonal	monoclinic
space group	$I4_1/acd$	$P2_1/c$
a [Å]	21.8924(7)	12.0391(14)
b [Å]	21.8924(7)	15.756(2)
c [Å]	32.8309(8)	14.3507(18)
α [deg]	90	90
β [deg]	90	94.045(11)
γ [deg]	90	90
V [Å^3]	15735.1(8)	2715.3(6)
$\rho_{calcd.}$ [gcm^{-3}]	2.045	1.814
Z	16	4
diffractometer (scan)	Nonius KappaCCD area detector ϕ and ω scan	Nonius KappaCCD area detector ϕ and ω scan
radiation	Mo Kα (graphite mon.)	Mo Kα (graphite mon.)
wavelength [Å]	0.71073	0.71073
F(000)	9280	1452
θ range [deg]	1.81 to 25.12	3.13 to 25.00
index ranges	$-25 \le h \le 22$ $-26 \le k \le 26$ $-38 \le l \le 39$	$-14 \le h \le 14$ $-18 \le k \le 18$ $-17 \le l \le 17$
no. of measd reflns	12 483	31 699
no. of unique reflns	2952	4656
no. of obsd reflns [$I_o > 2\sigma(I_o)$]	2406	3811
no. of refined params	259	384
goodness-of-fit on F^2	1.029	1.110
R [$I_o > 2\sigma(I_o)$]	0.0436	0.0381
wR_2 [all data]	0.1142	0.1285
ρ_{fin}(max./min.) [e Å^{-3}]	2.222/−1.219	1.969/−2.221

Bpa-Me,[21] bpa-Bz,[2] and $[\{(coe)_2Ir(\mu\text{-}Cl)\}_2]$[40] were prepared according to literature procedures. All other chemicals are commercially available and were used without further purification, unless stated otherwise.

X-ray Diffraction. A Nonius KappaCCD with area detector, φ and ω scans, was used, applying graphite-monochromatized Mo Kα radiation. The structures were solved by the program system DIRDIF[41] using the program PATTY[42] to locate the heavy atoms. The structure was refined with standard methods (refinement against F^2 of reflections with $I_o > 2\sigma(I_o)$ using SHELXL97[43]). Selected bond lengths and angles are summarized in Tables 1 and 2. Drawings were generated with the program PLATON.[44] Other relevant crystal data are summarized in Table 4.

$[\{(mer\text{-}\mu_2\text{-}bpa^{\#})Ir^{III}(C_2H_5)(CH_3CN)\}_2](PF_6)_2$, $4(PF_6)_2$. Crystals suitable for an X-ray structure determination were obtained from vapor diffusion of diethyl ether into an acetonitrile solution at rt. A single crystal was mounted in air on a glass fiber. Intensity data were collected at 150 K. Unit cell dimensions were determined from the angular setting of 12 483 reflections. All non-hydrogen atoms were refined with anisotropic temperature factors, except C4A and C4B. The hydrogen atoms were placed at calculated positions and refined isotropically in riding mode.

The compound crystallizes in the rather highly symmetrical space group $I4_1/acd$. The dinuclear iridium complex forms a dimer around an inversion center. The end-of-chain carbon atom C4 is disordered and has been split up over two separate positions. However, it proved to be impossible to refine these two positions anisotropically. The hydrogen atoms calculated on C4A, C4B, and C3 should be considered unreliable.

The space group has a multiplicity of the general position of 32, and thus the cell unit contains 16 molecules ($Z = 16$), $C_{32}H_{40}N_8Ir_2 \cdot 2(PF_6)$. The P atoms of the PF_6 moieties occupy three special positions, and especially the PF_6 moieties around P2 and P3 are highly disordered and should be considered very unreliable. Lowering the symmetry did not solve any of the problems described here. On the contrary, various atoms got unacceptable thermal displacement parameters (nonpositive definite) or could not be located at all in the Fourier map. Geometrical calculations with PLATON[43] revealed neither unusual geometric features nor unusual short intermolecular contacts. The calculations revealed no higher symmetry and no (further) solvent accessible areas.

$[\{(bpa\text{-}Bz^{\#})Ir^{III}(H)\}_2](PF_6)_2$, $5(PF_6)_2$. Crystals suitable for X-ray diffraction of this same compound were obtained when an acetone solution of $\mathbf{3}^+$ was allowed to stand at rt for three weeks. A single crystal was mounted in air on a glass fiber. Intensity data were collected at 208 K. Unit cell dimensions were determined from the angular setting of 31 699 reflections. All non-hydrogen atoms were refined with anisotropic temperature factors. The hydrogen atoms were placed at calculated positions and refined isotropically in riding mode. The structure consists of the Ir complex dimerized via an inversion center, two acetone moieties, and a rather disordered PF_6 moiety. The Ir−Ir distance is 2.6877(6) Å. Geometrical calculations with PLATON[43] revealed neither unusual geometric features nor unusual short intermolecular contacts. The calculations revealed no higher symmetry and no (further) solvent accessible areas.

(40) Herde, J. L.; Lambert, J. C.; Senoff, C. V. *Inorg. Synth.* **1974**, *15*, 18−20.

(41) Beurskens, P. T.; Beurskens, G.; Bosman, W. P.; de Gelder, R.; García-Granda, S.; Gould, R. O.; Israël, R.; Smits, J. M. M. *DIRDIF-96. A computer program system for crystal structure determination by Patterson methods and direct methods applied to difference structure factors*; Laboratory of Crystallography, Department of Inorganic Chemistry, University of Nijmegen: The Netherlands, 1996.

(42) Beurskens, P. T.; Beurskens, G.; Strumpel, M.; Nordman, C. E. *Patterson and Pattersons*, Glusker, J. P., Patterson, B. K., Rossi, M., Vol. Eds.; Clarendon Press: Oxford, 1987; p 356.

(43) Sheldrick, G. M. *SHELXL-97. Program for the refinement of crystal structures*; University of Göttingen: Germany, 1997.

(44) Spek, A. L. *PLATON-93. Program for display and analysis of crystal and molecular structures*; University of Utrecht: The Netherlands, 2003.

Synthesis. [(κ^3-bpa)Ir^I(C_2H_4)$_2$]PF_6, 1(PF_6). [Ir(coe)$_2$(μ-Cl)]$_2$ (155 mg, 0.17 mmol) was dissolved in 5 mL of methanol, and ethene was bubbled through the solution at room temperature until a clear solution was obtained. Under ethene atmosphere a solution of 120 mg (0.60 mmol, about 1.7 equiv) of bpa-H in 1,5 mL of methanol was added, and the mixture was stirred for a few minutes while bubbling through ethene. Subsequently 100.0 mg (0.54 mmol) of KPF_6 was added and the solution was stirred for 45 min under an ethene atmosphere. The solution was cooled to −78 °C to allow precipitation of **1**(PF_6). The thus obtained yellow-green solid was collected by filtration, washed three times with ice-cold methanol under a nitrogen atmosphere, and dried under vacuum. Yield: 115 mg (0.20 mmol, 61%). This complex was also synthesized using 70 mg (0.43 mmol) of NH_4PF_6 instead of KPF_6.

^{1}H NMR (400.15 MHz, CD_3CN, T = 298 K): δ (ppm) 7.73 (dt, 2H, J(H,H)$_{triplet}$ = 7.82 Hz and J(H,H)$_{doublet}$ = 1.71 Hz, Py-*H4*), 7.63 (d, 2H, J(H,H) = 5.62 Hz, Py-*H6*), 7.31 (d, 2H, J(H,H) = 7.82 Hz, Py-*H3*), 7.38 (s, 1H, N-*H*), 7.11 (t, 2H, J(H,H) = 6.72 Hz, Py-*H5*), 4.99 (dd[AB], 2H, J(H,H) = 15.76 Hz and J(H,H) = 5.50 Hz, Py-CH^AH-N), 4.65 (dd[AB], 2H, J(H,H) = 16.13 Hz and J(H,H) = 10.26, Py-CHH^B-N), 3.02 (t, 2H, J(H,H) = 10.14 Hz, $C_2H_4{}^A$), 2.89 (t, 2H, J(H,H) = 9.53 Hz, $C_2H_4{}^B$), 1.77 (t, 2H, J(H,H) = 9.53 Hz, $C_2H_4{}^B$ and $C_2H_4{}^A$). ^{13}C{^{1}H} NMR (50.03 MHz, CD_3CN, T = 298 K): δ (ppm) 167.54 (s, 2C, Py-*C2*), 150.58 (s, 2C, Py-*C6*), 138.53 (s, 2C, Py-*C4*), 126.29 (s, 2C, Py-*C3*), 123.08 (s, 2C, Py-*C5*), 60.97 (s, 2C, Py-CH_2−N), 36.64 (s, 2C, C_2H_4), 31.01 (s, 1C, $C_2H_4{}^A$), 25.61 (s, 1C, $C_2H_4{}^B$). ESI$^+$-MS: *m/z* 448 **1**$^+$, 420 {**1**−C_2H_4}$^+$, 392 {**1**−2*C_2H_4}$^+$. Anal. Calcd for $C_{16}H_{21}N_3IrPF_6$: C 32.43, H 3.57, N 7.09. Found: C 32.25, H 3.55, N 6.99.

[(κ^3-bpa-Me)Ir^I(C_2H_4)$_2$]PF_6, 2(PF_6). [Ir(coe)$_2$(μ-Cl)]$_2$ (150 mg, 0.17 mmol) was dissolved in 5 mL of methanol, and ethene was bubbled through the solution at room temperature until a clear solution was obtained. Under ethene atmosphere a solution of 71 mg (0.33 mmol) of bpa-Me in 1.5 mL of methanol was added, and the mixture was stirred for a few minutes while bubbling through ethene. Subsequently 80.0 mg (0.43 mmol) of KPF_6 was added, and the solution was stirred for 45 min under an ethene atmosphere. The solution was cooled to −78 °C to allow precipitation of **2**(PF_6). The thus obtained light green solid was collected by filtration, washed three times with ice-cold methanol under a nitrogen atmosphere, and dried under vacuum. Yield: 66.8 mg (0.11 mmol, 33%).

^{1}H NMR (400.15 MHz, CD_3CN, T = 298 K): δ (ppm) 7.79 (dt, 2H, J(H,H)$_{triplet}$ = 7.68 Hz and J(H,H)$_{doublet}$ = 1.63 Hz, Py-*H4*), 7.70 (d, 2H, J(H,H) = 5.62 Hz, Py-*H6*), 7.40 (d, 2H, J(H,H) = 8.30 Hz, Py-*H3*), 7.19 (t, 2H, J(H,H) = 6.72 Hz, Py-*H5*), 4.98 (d[AB], 2H, J(H,H) = 15.15 Hz, Py-CHH^B-N), 4.78 (d[AB], 2H, J(H,H) = 15.39 Hz, Py-CH^AH-N), 3.32 (t, 2H, J(H,H) = 10.14 Hz, $C_2H_4{}^A$), 3.18 (s, 3H, N-CH_3), 3.03 (t, 2H, J(H,H) = 9.65 Hz, $C_2H_4{}^B$), 1.87 (t, 2H, J(H,H) = 9.65 Hz, $C_2H_4{}^B$), 1.76 (t, 2H, J(H,H) = 9.77 Hz, $C_2H_4{}^A$). ^{13}C{^{1}H} NMR (50.03 MHz, CD_3CN, T = 298 K): δ (ppm) 166.07 (s, 2C, Py-*C2*), 150.40 (s, 2C, Py-*C6*), 138.67 (s, 2C, Py-*C4*), 126.62 (s, 2C, Py-*C5*), 124.61 (s, 2C, Py-*C3*), 71.05 (s, 2C, Py-CH_2-N), 53.81 (s, 1C, N-CH_3), 39.67 (s, 1C, $C_2H_4{}^A$), 36.38 (s, 1C, $C_2H_4{}^A$), 33.97 (s, 1C, $C_2H_4{}^B$), 28.53 (s, 1C, $C_2H_4{}^B$). ESI$^+$-MS: *m/z* 462 **2**$^+$, 434 {**2**−C_2H_4}$^+$, 406 {**2**−2*C_2H_4}$^+$. Anal. Calcd for $C_{17}H_{23}N_3IrPF_6$: C 33.66, H 3.82, N 6.93. Found: C 33.72, H 3.86, N 7.07.

[(κ^3-bpa-Bz)Ir^I(C_2H_4)$_2$]PF_6, 3(PF_6). [Ir(coe)$_2$(μ-Cl)]$_2$ (150 mg, 0.17mmol) was dissolved in 5 mL of methanol, and ethene was bubbled through the solution at room temperature until a clear solution was obtained. Under ethene atmosphere a solution of 97 mg (0.34 mmol) of bpa-Bz in 1.5 mL of methanol was added and stirred for a few minutes while bubbling through ethene. Subsequently 80.0 mg (0.43 mmol) of KPF_6 was added, and the solution was stirred for 45 min under an ethene atmosphere. The solution was cooled to −78 °C to allow precipitation of **3**(PF_6). The thus obtained light yellow solid was collected by filtration, washed three times with ice-cold methanol under a nitrogen atmosphere, and dried under vacuum. Yield: 123.7 mg (0.18 mmol, 54%).

^{1}H NMR (400.15 MHz, CD_2Cl_2, T = 298 K): δ (ppm) 7.85 (t, 2H, J(H,H) = 7.77 Hz, Py-*H4*), 7.70 (d, 2H, J(H,H) = 5.57 Hz, Py-*H6*), 7.58 (m, 3H, Ph-*H3*, Ph-*H4* and Ph-*H5*), 7.50 (d, 2H, J(H,H) = 7.92 Hz, Py-*H3*), 7.24 (m, 4H, Py-*H5*, Ph-*H2* and Ph-*H6*), 5.39 (s, 4H, free C_2H_4), 5.10 (d[AB], 2H, J(H,H) = 15.53 Hz, Py-CH^AH-N), 4.64 (d[AB], 2H, J(H,H) = 15.68 Hz, Py-CHH^B-N), 4.36 (s, 2H, N-CH_2-Ph), 3.44 (t, 2H, J(H,H) = 10.11 Hz, $C_2H_4{}^A$), 3.27 (t, 2H, J(H,H) = 9.67 Hz, $C_2H_4{}^B$), 2.03 (t, 2H, J(H,H) = 9.67 Hz, $C_2H_4{}^B$), 1.94 (t, 2H, J(H,H) = 9.89 Hz, $C_2H_4{}^A$). ^{13}C{^{1}H} NMR (50.03 MHz, CD_3CN, T = 298 K): δ (ppm) 165.62 (s, 2C, Py-C2), 150.65 (s, 2C, Py-C6), 138.97 (s, 2C, Py-C4), 133.32 (s, 2C, Ph-C2, Ph-C6), 132.25 (s, 1C, Ph-C1), 130.04 (d, 3C, Ph-C3, Ph-C4, Ph-C5), 126.82 (s, 2C, Py-C5), 125.04 (s, 2C, Py-C3), 64.92 (s, 1C, Ph-CH_2-N), 64.47 (s, 2C, Py-CH_2-N), 35.00 (s, 2C, $C_2H_4{}^A$), 30.60 (s, 2C, $C_2H_4{}^B$). ESI$^+$-MS: *m/z* 538 **3**$^+$, 510 {**3**−C_2H_4}$^+$, 482 {**3**−2·C_2H_4}$^+$. Anal. Calcd for $C_{23}H_{27}N_3IrPF_6$: C 40.47, H 3.99, N 6.16. Found: C 40.53, H 4.03, N 6.05.

[{(*mer*-μ_2-bpa$^\#$)Ir^{III}(C_2H_5)(CH_3CN)}$_2$](PF_6)$_2$, 4(PF_6)$_2$. (bpa$^\#$ = *N*,*N*-di(2-pyridylmethyl)amine (=bpa) with the amine-nitrogen deprotonated.) **1**(PF_6) (115 mg, 0.19 mmol) was dissolved in acetonitrile and heated to approximately 70 °C under stirring for 2 h. The solvent was removed, and the product was analyzed. In another experiment **1**(PF_6) was dissolved in acetonitrile-d_3 and left standing at room temperature for 2 weeks. Here also product **4**(PF_6)$_2$ was formed. Crystals, suitable for X-ray diffraction, were obtained by vapor diffusion of diethyl ether into a solution of **4**(PF_6)$_2$ in acetonitrile. Yield: 73.5 mg (81.5%).

^{1}H NMR (400.15 MHz, CD_3CN, T = 298 K): δ (ppm) 8.49 (d, 4H, J(H,H) = 5.08 Hz, Py-*H6*), 7.50 (dt, 4H, J(H,H)$_{triplet}$ = 7.80 Hz, J(H,H)$_{doublet}$ = 1.49 Hz, Py-*H4*), 7.08 (t, 4H, J(H,H) = 6.54 Hz, Py-*H5*), 6.84 (d, 4H, J(H,H) = 7.84 Hz, Py-*H3*), 4.75 (d[AB], 4H, J(H,H) = 17.57 Hz, Py-CHH^B-N), 4.62 (d[AB], 4H, J(H,H) = 17.57, Py-CH^AH-N), 2.70 (s, 6H, coordinated CH_3-CN), 1.06 (q, 4H, J(H,H) = 7.63 Hz, −CH_2CH$_3$), 0.01 (t, 6H, J(H,H) = 7.62 Hz, −CH_2CH_3). ^{13}C{^{1}H} NMR (50.03 MHz, CD_3-CN, T = 298 K): δ (ppm) 172.39 (s, 4C, Py-*C2*), 150.39 (s, 4C, Py-*C6*), 137.66 (s, 4C, Py-*C4*), 124.96 (s, 4C, Py-*C5*), 122.73 (s, 4C, Py-*C3*), 119.02 (s, 2C, coordinated CH_3CN), 69.36 (s, 4C, Py-CH_2-N), 15.10 (s, 2C, −CH_2CH_3), 4.78 (s, 2C, coordinated CH_3CN), −10.29 (s, 2C, −CH_2CH_3). ESI$^+$-MS: *m/z* 463.5 [**4**]$^{2+}$. Anal. Calcd for $C_{33}H_{43}N_9Ir_2P_2F_{12}$ ([**4**](PF_6)$_2$·CH_3CN): C, 32.61; H, 3.46; N, 10.07. Found: C, 32.62; H, 3.31; N, 9.87.

[{(κ^4-*C*,*N*,*N*′-bpa-Bz)Ir^{III}(μ_2-H)}$_2$]PF_6 (or [{(bpa-Bz$^\#$)Ir^{III}-(μ_2-H)}$_2$]PF_6, 5(PF_6)$_2$). (bpa-Bz# = *N*-benzyl-*N*,*N*-di(2-pyridylmethyl)amine (=bpa-Bz) with the benzyl ring deprotonated at C2.) A saturated solution of 100 mg (0.15 mmol) of **3**$^+$ in 15 mL of acetone was heated to 50 °C for about 3 days, leading to precipitation of **5**(PF_6)$_2$ as a fine, light yellow powder. The powder was separated from the solution and subsequently washed twice with acetone at −30 °C. Yield: 33.6 mg (0.027 mmol, 18%). The phenyl group is cyclometalated at C2.

^{1}H NMR (400.14 MHz, acetone-d_6, 298 K): δ (ppm) 7.94 (td, 4H, J(H,H)$_{doublet}$ = 5.68 Hz, J(H,H)$_{triplet}$ = 1.16 Hz, Py-*H6*), 7.8−7.7 (m, 8H, Py-*H3* and -*H4*), 7.55 (dd, 2H, J(H,H) = 7.42 Hz, J(H,H) = 0.96 Hz, Ph-*H3*), 6.65 (dt, 2H, J(H,H)$_{triplet}$ = 9.56 Hz, J(H,H)$_{doublet}$ = 1.56 Hz, Ph-*H4*), 6.62 (m, 4H, Py-*H5*), 6.58 (dt, 2H, J(H,H)$_{triplet}$ = 7.40 Hz, J(H,H)$_{doublet}$ = 1.36 Hz, Ph-*H5*), 6.45 (dd, 2H, J(H,H) = 7.14 Hz, J(H,H) = 1.00 Hz, Ph-*H6*), 6.15 (d[AB], 4H, J(H,H) = 14.85 Hz, N-CH_2-Py), 5.64 (d[AB], 4H, J(H,H) = 15.05 Hz, N-CH_2-Py), 4.67 (s, 4H, N-CH_2-Ph), −14.73 (s, 2H, Ir-*H*-Ir). Due to the extremely low solubility in acetone-d_6, it was not possible to measure a ^{13}C NMR spectrum. However, it was possible to measure gHSQC and gHMBC (C−H correlation spectra), from which some of the ^{13}C chemical shifts could be deduced. ^{13}C{^{1}H} NMR (50.03 MHz, acetone-d_6, 298 K): δ (ppm) 166.1 (Py-C2), 155.8 (Py-

C6), 148.8 (Ph-*C2*), 138.64 (Ph-*C3*), 138.52 (Py-*C3* or -*C4*), 134.9 (Ph-*C1*), 126.73 (Py-*C5*), 126.40 (Ph-*C4*), 124.69 (Py-*C3* or -*C4*), 124.40 (Ph-*C5*), 119.87 (Ph-*C6*), 73.45 (N-*C*H_2-Py), 68.52 (N-*C*H_2-Ph). ESI$^+$-MS (acetone-d_6 solution diluted with acetone): *m/z* 481 $\mathbf{5}^{2+}$ (dicationic dinuclear complex), 482 [(bpa-Bz$^{\#}$)Ir(H)]$^+$ (monocationic, monomeric complex), 540 [(bpa-Bz$^{\#}$)-Ir(H)(acetone)]$^+$. Anal. Calcd for $C_{38}H_{38}N_6Ir_2P_2F_{12}$: C, 36.42; H, 3.06; N, 6.71. Found: C, 36.25; H, 3.12; N, 6.81.

[(κ^4-*C,N,N′*-bpa-Bz)Ir^{III}(H)(CD$_3$CN)]PF$_6$ (or [(bpa-Bz$^{\#}$)-Ir^{III}(H)(CD$_3$CN)]PF$_6$, 6(PF$_6$)). Upon dissolving $\mathbf{3}^+$ in CD_3CN, conversion to $\mathbf{6}^+$ takes place very rapidly. After 25 min only 13% of the original dinuclear complex is left. Within a few hours, full conversion to $\mathbf{6}^+$ takes place. The phenyl group is cyclometalated at C2.

^{1}H NMR (400.14 MHz, CD_3CN, 298 K): δ (ppm) 8.66 (dd, 2H, J(H,H) = 5.60 Hz, J(H,H) = 0.48 Hz, Py-*H6*), 7.74 (dt, 2H, $J(H,H)_{triplet}$ = 7.82 Hz, $J(H,H)_{doublet}$ = 1.68 Hz, Py-*H4*), 7.65 (d, 1H, J(H,H) = 7.58 Hz, Ph-*H3*), 7.40 (dd, 2H, J(H,H) = 7.84 Hz, J(H,H) = 0.48 Hz, Py-*H3*), 7.08 (mt, 2H, J(H,H) = 8.56 Hz, Py-*H5*), 6.68−6.63 (m, 1H, Ph-*H4*), 6.60 (dt, $J(H,H)_{triplet}$ = 7.56 Hz, $J(H,H)_{doublet}$ = 1.48 Hz, Ph-*H5*), 6.58 (m, 1H, Ph-*H6*), 5.09 (d[AB], 2H, J(H,H) = 15.41 Hz, N-CH_2-Py), 5.02 (d[AB], 2H, J(H,H) = 15.41 Hz, N−CH_2−Py), 4.47 (s, 2H, N-CH_2-Ph), −18.30 (s, 1H, Ir-H). ^{13}C{^{1}H} NMR (50.03 MHz, CD_3CN, 298 K): δ (ppm) 166.89 (s, Py-*C2*), 158.23 (s, Py-*C6*), 149.85 (s, Ph-*C2*), 139.56 (s, Ph-*C1*), 142.17 (s, Ph-*C3*), 138.04 (s, Py-*C4*), 126.64 (s, Ph-*C4*), 126.46 (s, Py-*C5*),124.08 (s, Py-*C3*), 123.02 (s, Ph-*C5*), 120.14 (s, Ph-*C6*), 69.92 (s, N-CH_2-Py), 69.75 (s, N-CH_2, Ph). ESI$^+$-MS (CD_3CN solution diluted with CH_3-CN) [(bpa-Bz$^{\#}$)Ir^{III}(H)(CH_3CN)]$^+$: *m/z* 523 $\mathbf{6}^+$, 482 {$\mathbf{6}$−CH_3-CN}$^+$. Anal. Calcd for $C_{21}H_{22}IrN_4$: 523.14745. Found: 523.14433 (Δ = −5.8 ppm). [(bpa-Bz$^{\#}$)Ir^{III}(H)(CH_3CN)]$^+$: *m/z* 526 $\mathbf{6}^+$, 482 {$\mathbf{6}$−CD_3CN}$^+$. Anal. Calcd for $C_{21}H_{19}IrN_4D_3$: 526.16626. Found: 526.16337 (Δ = −5.3 ppm).

[(bpa-Bz$^{\#}$)Ir^{III}(μ^2-H)Ir(H)(bpa-Bz$^{\#}$)](PF$_6$)$_2$, 7(PF$_6$)$_2$. Complex $\mathbf{7}^{2+}$ was obtained as the only product by exposing an acetone-d_6 solution of $\mathbf{5}^+$ for about 5 h to glass-filtered light. The phenyl group is cyclometalated at C2. Py, Py″, and Ph′ belong to the asymmetrically coordinated N_3 ligand and Py′, Py‴, and Ph belong to the symmetrically coordinated N_3 ligand.

^{1}H NMR (400.14 MHz, acetone-d_6, 298 K): δ (ppm) 9.22 (d, 1H, J(H,H) = Hz, Py‴-*H6*), 8.11 (td, ^{1}H, $J(H,H)_{doublet}$ = 5.36 Hz, $J(H,H)_{triplet}$ = 1.20 Hz, Py-*H6*), 7.95 (m, 1H, Py′-*H6*), 7.88−7.85 (m, 2H, Py-*H3* and -*H4*), 7.81−7.78 (m, 2H, Py′-*H3* and -*H4*), 7.72−7.66 (m, 3H, Py‴-*H3* and *H4*, Py″-*H4*), 7.38 (td, ^{1}H, $J(H,H)_{doublet}$ = 5.64 Hz, $J(H,H)_{triplet}$ = 0.96 Hz, Py″-*H6*), 7.23 (dd, J(H,H) = 7.68 Hz, J(H,H) = 1.20 Hz, Ph-*H3*), 7.21−7.15 (m, 2H, Py″-*H3*, Py‴-*H5*), 7.08 (d, ^{1}H, J(H,H) = 7.32 Hz, Ph′-*H6*), 6.9 (m, 1H, Py-*H5*), 6.69 (m, 1H, Py′-*H5*), 6.66 (m, 1H, Ph-*H4*), 6.65−6.55 (m, 3H, Py″-*H5*, Ph-*H5*, Ph′-*H5*), 6.52 (dd, ^{1}H, J(H,H) = 7.58 Hz, J(H,H) = 1.00 Hz, Ph′-*H3*), 6.39 (dd, ^{1}H, J(H,H) = 7.32 Hz, J(H,H) = 1.24 Hz, Ph-*H6*), 6.2−6.1 (m, 2H, N-CH_2-Py′ and Ph′-*H4*, 6.01 (d[AB]^{Py} and Py‴, 1H, J(H,H) = 16.61 Hz, N-CH_2-Py and -Py‴), 5.67 (d[AB]$^{Ph'}$, 1H, J(H,H) = 12.68 Hz, N-CH_2-Ph′), 5.61 (d[AB]^{Py}, 1H, J(H,H) = 14.93 Hz, N-CH_2-Py), 5.36 (d[AB]$^{Py'}$, 1H, J(H,H) = 14.89 Hz, N-CH_2-Py′), 5.30 (d[AB]$^{Py'''}$, 1H, J(H,H) = 14.65 Hz, N-CH_2-Py‴), 5.20 (d[AB]$^{Ph'}$, 1H, J(H,H) = 12.96 Hz, N-CH_2-Ph′), 4.95 (d[AB]$^{Py''}$, 1H, J(H,H) = 19.29 Hz, N-CH_2-Py″), 4.88 (d[AB]$^{Py''}$, 1H, J(H,H) = 19.05 Hz, N-CH_2-Py″), 4.63 (s, 2H, N-CH_2-Ph), −14.90 (s, 1H, Ir-*H*-Ir), −23.92 (s, 1H, Ir-*H′*-Ir). Due to the extremely low solubility in acetone-d_6, it was not possible to measure a ^{13}C NMR spectrum. ESI$^+$-MS (actone-d_6 solution diluted with acetone): *m/z* 481 $\mathbf{7}^{2+}$ (dicationic dinuclear complex), 482 [(bpa-Bz$^{\#}$)Ir(H)]$^+$ (monocationic, monomeric complex), 540 [(bpa-Bz$^{\#}$)Ir(H)(acetone)]$^+$. In contrast with $\mathbf{5}^+$ much less [(bpa-Bz$^{\#}$)Ir(H)]$^+$ is present in the mass spectrum, indicating a much more strongly bound dinuclear complex. ESI$^+$-MS (acetone-d_6/CD_3CN solution diluted with CH_3CN): *m/z* 481 $\mathbf{7}^{2+}$, 503 {$\mathbf{7}$(CD_3CN)}$^{2+}$, 523 [(bpa-Bz$^{\#}$)Ir(H)(CH_3CN)]$^+$, 526 [(bpa-Bz$^{\#}$)Ir(H)(CD_3CN)]$^+$. In contrast with previous ESI$^+$-MS measurements of $\mathbf{5}^+$ and $\mathbf{7}^+$ in acetone, no [(bpa-Bz$^{\#}$)Ir-(H)(solvent)]$^+$ and hardly any [(bpa-Bz$^{\#}$)Ir(H)]$^+$ is present in the spectrum.

Acknowledgment. This work was supported by the Dutch National Science Foundation (NWO). We thank Dr. Peter H. M. Budzelaar for helpful discussions.

Supporting Information Available: Crystallographic data in CIF format. This material is available free of charge via the Internet at http://pubs.acs.org.

OM050594K